DOI: 10.1002/chem.200903525

DFT Mechanistic Study on Diene Metathesis Catalyzed by Ru-Based Grubbs–Hoveyda-Type Carbenes: The Key Role of π-Electron Density Delocalization in the Hoveyda Ligand

Xavier Solans-Monfort,* Roser Pleixats, and Mariona Sodupe[a]

Abstract: The catalytic activity and catalyst recovery of two heterogenized ruthenium-based precatalysts (**H** and **NO_2(4)**) in diene ring-closing metathesis have been studied by means of density functional calculations at the B3LYP level of theory. For comparison and rationalization of the key factors that lead to higher activities and higher catalyst recoveries, four other Grubbs–Hoveyda complexes have also been investigated. The full catalytic cycle (catalyst formation, propagation, and precatalyst regeneration) has been considered. DFT calculations suggest that either for the homogeneous and heterogenized systems the activity of the catalysts mainly depends on the ability of the precursor to generate the propagating carbene. This ability does not correlate with the traditionally identified key factor, the Ru···O interaction strength. In contrast, precatalysts with lower alkoxy-dissociation energy barriers and lower stabilities compared with the propagating carbene also present larger C1−C2 bond length (i.e., lower π character of the C−C bond that exists between the metal–carbene (Ru=C) and the phenyl ring of the Hoveyda ligand). Catalyst recovery, regardless of whether a release–return mechanism occurs or not, is also mainly determined by the π delocalization. Therefore, future Grubbs–Hoveyda-type catalyst development should be based on fine-tuning the π-electron density of the phenyl moiety, with the subsequent effect on the metalloaromaticity of the ruthenafurane ring, rather than considering the modification of the Ru···O interaction.

Keywords: density functional calculations · diene ligands · metathesis · pi interactions · ruthenium

Introduction

Olefin metathesis is a very versatile reaction for the formation of carbon–carbon double bonds even in the presence of other functional groups.[1–8] This makes the process a very powerful tool in organic synthesis; the number of applications increases every day. The reaction requires the presence of a suitable catalyst, which can be a transition-metal oxide (MoO_3, WO_3, or Re_2O_7) supported on silica, alumina, or magnesia,[7,9] or a well-defined organometallic complex.[1,2,4,10–14] Two main groups of molecular catalysts can be distinguished: 1) the d^0 early-transition-metal carbenes of general formula $[M(\equiv NR^1)(=CHR^2)(X)(Y)]$, in which M is usually Mo or W and $X=Y=OR^3$ (a Schrock-type catalyst, **1** in Scheme 1),[4,10] and 2) the Ru-based carbenes of general formula $[Ru(Cl)_2(=CHR^1)(L^1)(L^2)]$,[1,2,6] in which L^1 is a phosphine ligand in the so-called first-generation Grubbs catalyst[11] (**2** in Scheme 1) or a N-heterocyclic carbene (NHC) in the second-generation Grubbs catalyst[12] (**3** in Scheme 1). One particular case of second-generation complexes is the Grubbs–Hoveyda catalyst ($\mathbf{H_M}$ in Scheme 1).[13,14] Second-generation catalysts, that is, complexes with an NHC ligand, usually present higher activities

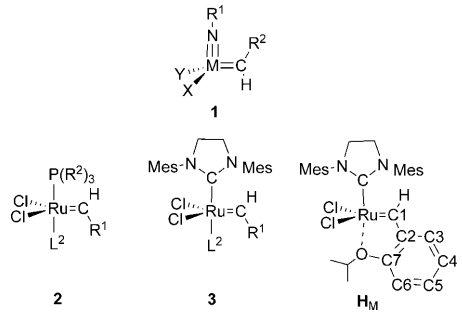

Scheme 1.

[a] Dr. X. Solans-Monfort, Prof. R. Pleixats, Prof. M. Sodupe
Departament de Química, Universitat Autònoma de Barcelona
08193 Cerdanyola del Vallès (Spain)
Fax: (+34) 935812920
E-mail: xavi@klingon.uab.cat

Supporting information for this article is available on the WWW under http://dx.doi.org/10.1002/chem.200903525.

(higher conversions per unit of time) and this has been reported to depend on the compromise between L^2 dissociation (easier for first-generation complexes) and the facility of subsequent olefin coordination (favored for second-generation complexes).[1,15,16]

Heterogeneous catalysts are more robust and allow a much easier separation of products and catalyst. Therefore, they are the preferred choice in industrial applications. Nevertheless, they are generally not suitable for fine chemicals: they show low selectivities and in general they are not catalytically active when reactants contain other functional groups.[5,7] On the other hand, homogeneous catalysts have a well-defined structure, they work at lower temperatures, and they are able to catalyze metathesis reactions for a large variety of functionalized olefins.[5] Consequently, they show much higher selectivities that make them suitable for the synthesis of fine chemicals. Unfortunately, the fact that products and catalyst are in the same phase makes their separation more complex and it may lead to metal-contaminated products.

With the aim of combining the advantages of heterogeneous and homogeneous processes, many authors have synthesized well-defined heterogeneous catalysts by supporting organometallic complexes on different solids and surfaces such as oxides or polymers.[5,9,17,18] In this way, some of us have recently prepared several Grubbs–Hoveyda-type heterogenized catalysts through sol–gel procedures on suitably modified Hoveyda ligands (Scheme 2).[19–21] These catalysts

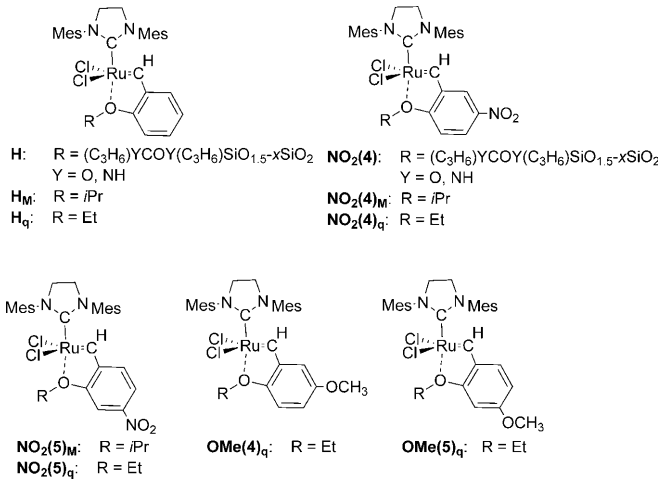

Scheme 2. Grubbs–Hoveyda-based precatalysts considered in the present work. Subscript M stands for molecular analogue and subscript q for computational (quantum) model.

present good activities in ring-closing diene and enyne metathesis. Interestingly, it has been observed that the nitro-substituted Grubbs–Hoveyda-based catalysts **NO_2(4)** (Scheme 2) require considerably lower reaction times to achieve full conversion in the first catalytic runs than the nonsubstituted catalysts **H**.[20,21] Nevertheless, the **NO_2(4)** catalyst showed a pronounced decrease of activity upon recycling, whereas **H** shows similar or only slightly lower activity after several runs.

These observations are in agreement with those trends observed for the homogeneous Grubbs–Hoveyda analogues.[22–24] The presence of electron-withdrawing substituents, such as the nitro group (**NO_2(4)$_M$** and **NO_2(5)$_M$**) in the phenyl ring of the chelating ligand leads to catalysts that generally achieve full reactant conversion in lower reaction times than the nonsubstituted Grubbs–Hoveyda catalyst, **H_M**. Moreover, the inclusion of electron-donor substituents, such as alkoxy groups (**O*i*Pr(4)$_M$** and **O*i*Pr(5)$_M$**),[23] leads to catalysts that require longer reaction times to achieve the same conversion as **H_M**. In this sense, Blechert and co-workers suggested that the inclusion of electron-withdrawing groups decreases the electron density either at the alkoxy group or on the Ru=C bond, thereby enhancing the catalytic activity.[23]

Moreover, regarding catalyst recovery, it has been reported that the Grubbs–Hoveyda catalyst **H_M** can be recovered up to a 95% after reaction by chromatography,[14] whereas the percentages of **NO_2(4)** complexes isolated after reaction are lower.[22]

Many theoretical works that focus on the olefin metathesis mechanism catalyzed either by heterogeneous,[25] homogeneous Schrock-type,[26–28] or Grubbs-type catalysts[29–36] can be found in the literature. For the particular case of Ru-based catalysts, calculations have allowed one to determine the most favorable reaction pathway based on Chauvin's mechanism,[37] but it adds an initial step associated with the creation of a vacant site at the metal center that involves the decoordination of the L^2 ligand (see Scheme 3).[29,32,34] Despite the fact that Grubbs–Hoveyda catalysts have been widely used experimentally,[1,8,13,14,22] to our knowledge they have only been briefly studied from a theoretical point of view,[36] and in particular, the factors that control the catalytic activity and recovery of these compounds have never been addressed.

In this context, the present work has three main goals: 1) to determine the origin of the higher catalytic activity of **NO_2(4)** compared to that of **H**; 2) to determine the factors that influence the catalyst recovery, and 3) to understand how the electronic nature and position of the substituents in the phenyl ring of the Hoveyda ligand affect the activity and recovery of the Grubbs–Hoveyda-type catalysts. The understanding of the role of each substituent can be the basis for further catalyst improvement.

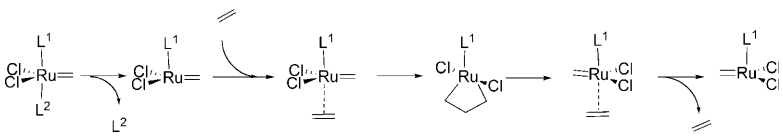

Scheme 3.

Computational details: The Grubbs–Hoveyda-type heterogenized catalysts (**H** and **NO_2(4)**) and the molecular analogues (**H_M**, **$NO_2(4)_M$**, **$NO_2(5)_M$**, **O*i*Pr(4)$_M$**, **O*i*Pr(5)$_M$**) have been represented by one set of molecular models (**X_q**) in which the actual bulk of the catalyst is included in the calculations except: 1) the anchoring ligand and the surface support, which are represented by an ethoxy (EtO) group, and 2) the O*i*Pr Hoveyda ligand substituents of catalysts **O*i*Pr(4)$_M$** and **O*i*Pr(5)$_M$** that have been simplified to OMe groups (Scheme 2). This kind of approach has been previously used in other heterogenized catalysts[38] and it assumes that the surface has very little electronic influence on the metal center. The reacting diene, *N*,*N*-diallyl-4-methylbenzenesulfonamide (**4**), has also been simplified to *N*,*N*-diallylmethanesulfonamide (**4_q**) (Scheme 4) to decrease the computational cost without losing significant electronic contributions.

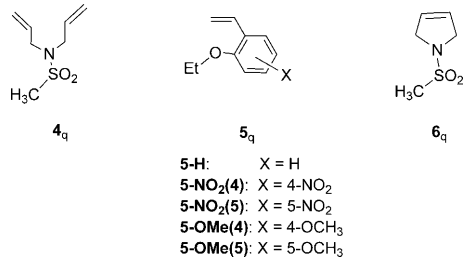

Scheme 4.

Calculations have been performed with the B3LYP[39] hybrid density functional as implemented in the Gaussian 03 package.[40] The optimized geometries have been obtained using basis set A (BSA), which consists of: 1) the quasi-relativistic effective core pseudopotentials (RECP) of the Stuttgart group[41] and the associated basis sets augmented with a polarization function[42] for Ru, that is, the 1s, 2s, 2p, 3s, 3p, and 3d electrons are included in the pseudopotential and the outer 4s, 4p, and 4d electrons are described with the (8s7p6d1f)/[6s5p3d1f] basis sets; and 2) the 6-31G(d,p)[43] basis set for all other atoms. The final energetics are obtained from single-point calculations at the BSA-optimized geometries, with a larger basis that includes diffuse functions for C, N, O, H, and S, namely, 6-31++G(d,p) (basis set B (BSB)).[43,44] The nature of all stationary points has been verified by vibrational analysis. In addition, for some transition states the intrinsic reaction coordinate (IRC) method has been performed to determine the interconnected minima. To ensure the accuracy of the present methodology, some test calculations using both M06L and M06X density functionals[45] have also been performed with the Gaussian 09 package.[46] These functionals better reproduce the dispersion forces and thus they have been suggested to be more reliable in reproducing some experiments on olefin metathesis.[16,47,48] In particular, we have compared the chelating ligand alkoxy-dissociation energy barriers and the relative energies of the precatalysts compared with the most stable intermediates that result from B3LYP calculations with those values obtained using the same procedure but M06L and M06X functionals. Energetics and geometries obtained with M06L and M06X are reported in Table S1 and Figure S1 of the Supporting Information. The absolute values are only slightly affected by the level of theory. M06L and M06X functionals lead to energy barriers that are between 3 to 4 kcal mol^{-1} higher in energy and to precursor stabilities that are around 5 to 9 kcal mol^{-1} higher. More interestingly, the same trends are obtained independently of the functional used.

Solvent effects have been included by performing single-point calculations at the gas-phase-optimized geometry using the polarizable continuum model (PCM)[49] and the experimentally used dichloromethane (CH_2Cl_2) as solvent.

The energetics reported in the manuscript are based on electronic energies plus solvation free energies, $E+\Delta G_{solv}$, and thus do not include the entropic contribution of the solute.[50] This leads to an overstabilization of those intermediates with lower molecularity,[50,51] and in particular of the metallacycle intermediates. Alternatively, one can consider energetics based on $G_{gp}+\Delta G_{solv}$ that includes the loss of rotation and translation on going from two molecules to one in the gas phase.[52,53] Nevertheless, it is well known that ΔS^{rot} and ΔS^{trans} are larger in the gas phase than in solution because rotation and translation in solution are much more constrained.[53–55] There is still no standard procedure in the literature but most of the theoretical works in catalysis and specially in olefin metathesis are based on $E+\Delta G_{solv}$.[29,31,32,35] That is, the nonexistence of a systematic way of calculating S^{rot}_{sol} and S^{trans}_{sol}, along with the accepted general idea that $G_{gp}+\Delta G_{solv}$ overestimates the entropic contribution of the solute much more than $E+\Delta G_{solv}$ underestimates it, precludes usually the inclusion of the gas-phase entropic corrections.[28,51,53,54]

Results and Discussion

Results are organized as follows. First, we present in detail the reactivity of **H_q** and **$NO_2(4)_q$** with **4_q** (Schemes 2 and 4). We have considered the global catalytic cycle (Scheme 5), which involves three processes:[18,56,57] A) the cross-metathesis that leads to the real catalyst generation; B) the propagation process, which corresponds to the ring-closing diene metathesis, and which is the same for all the catalysts presented here; and C) the cross-metathesis that leads to the catalyst precursor regeneration. In all cases, we have only considered the dissociative mechanism and the olefin coordination *trans* to the NHC ligand (Scheme 3) since previous studies have concluded that this is the preferred mechanism.[31–33,47] Afterwards, we analyze the effect of electron-donor and electron-withdrawing groups in the activity and catalyst recovery of several modified Grubbs–Hoveyda derivatives.

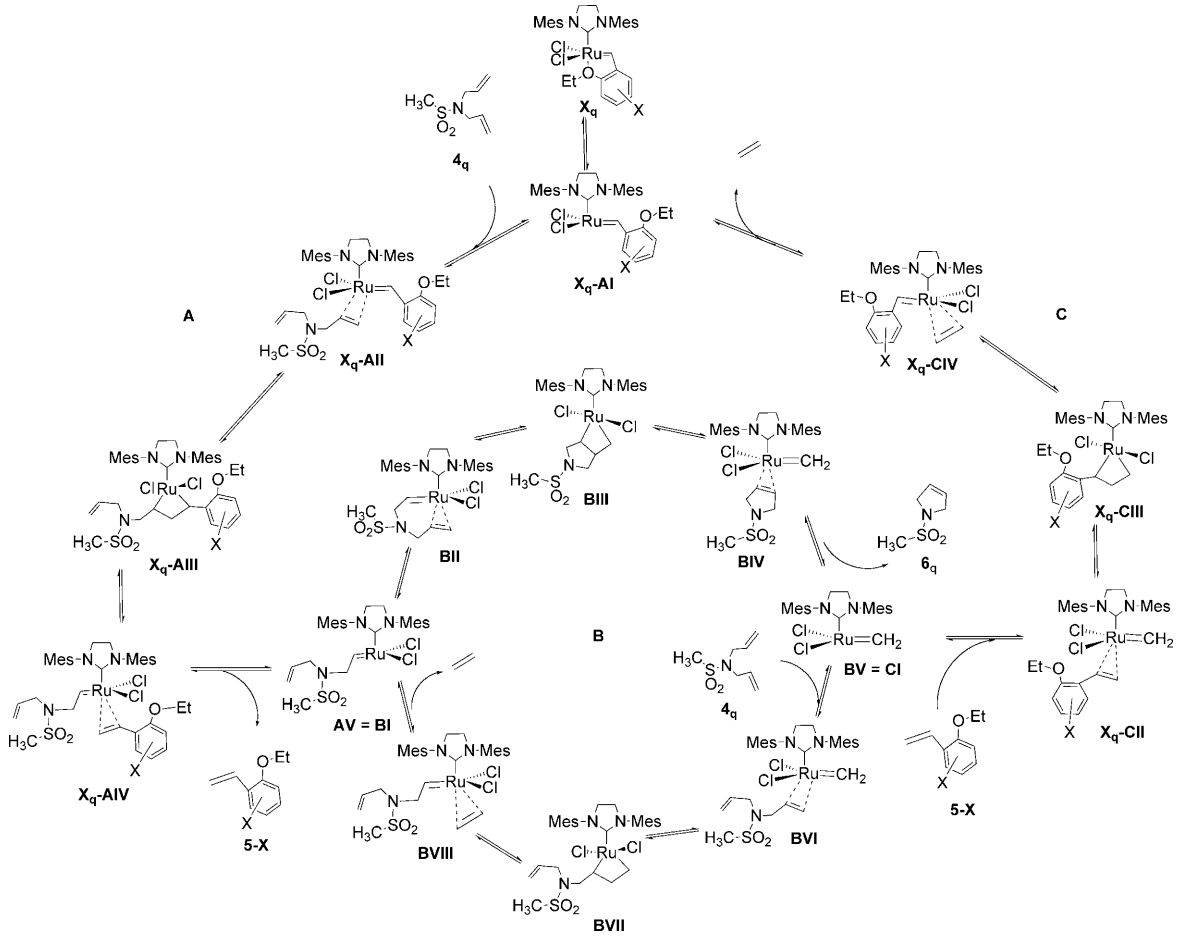

Scheme 5. Computed mechanism that consists of three different processes: A) catalyst generation, B) real catalytic cycle, and C) precatalyst regeneration. Part A and C imply heterogenized species, whereas the catalytic cycle B takes place in solution.

Catalytic activity of H_q and $NO_2(4)_q$: Figures 1, 2, and 3 show the energy profiles and some selected optimized geometries for catalyst generation (Figure 1), propagation (Figure 2), and catalyst precursor regeneration (Figure 3) associated with processes A, B, and C, respectively. It is worth noting that all relative energies are given with respect to the **BII+5-X** propagating carbene. This species is common to the two catalysts and thus allows easier comparison. Optimized structures of all intermediates and their Cartesian coordinates are given in Figures S2, S3, and S4 in the Supporting Information. The precursors, H_q and $NO_2(4)_q$, present a distorted square-based pyramidal (SBP) geometry, with the carbene ligand in the apical position (Figure 1) and the two chlorine ligands, the NHC, and the alkoxy group in the basal plane. The main deviation from the ideal SBP structure comes from a significantly closed Cl-Ru-Cl angle (156.2° for H_q and 154.4° for $NO_2(4)_q$). The smaller angle for $NO_2(4)_q$ correlates with a slightly shorter Ru=C bond. Variations are very small, but this relationship between the Ru=C bond length and the Cl-Ru-Cl angle opening is also observed for $NO_2(5)_q$, $OMe(4)_q$, and $OMe(5)_q$ (vide infra). Analysis of the molecular orbitals indicates that the ruthenium d orbital involved in the π Ru=C bond also has an antibonding character with the chlorine ligands. In this way, a stronger Ru=C π interaction produces a higher Ru−Cl π repulsion, which is minimized by closing the Cl-Ru-Cl angle. As expected, the Hoveyda ligand is planar and this leads to a planar ruthenafurane cycle. The computed geometry is in agreement with the available X-ray data of H_M[14] and other related complexes.[58] In particular, all calculated Ru=C and Ru−C_{NHC} distances are almost identical to the experimental ones, whereas the Ru−Cl and Ru···O distances obtained from calculations are slightly larger (less than 0.08 Å).

Dissociation of the alkoxy substituent of the Grubbs–Hoveyda ligand to create a vacant site occurs through a C1−C2 rotation (Scheme 1), which leads to a seesaw coordination around Ru with the alkoxy group pointing to the mesityl substituents (H_q-**AI**). Furthermore, the NHC and the carbene substituents remain in the same plane after the whole process. The transition-state structure presents the benzene ring almost perpendicular to the NHC plane, with an Ru-C1-C2-C3 torsion angle of 72.6° and an Ru···O distance of 3.550 Å, which suggest that the Ru···O interaction is already lost in the transition-state structure. Moreover, the Ru=C bond length is considerably shorter in the transition-state structure (1.814 Å) than in either H_q (1.829 Å) or H_q-**AI**

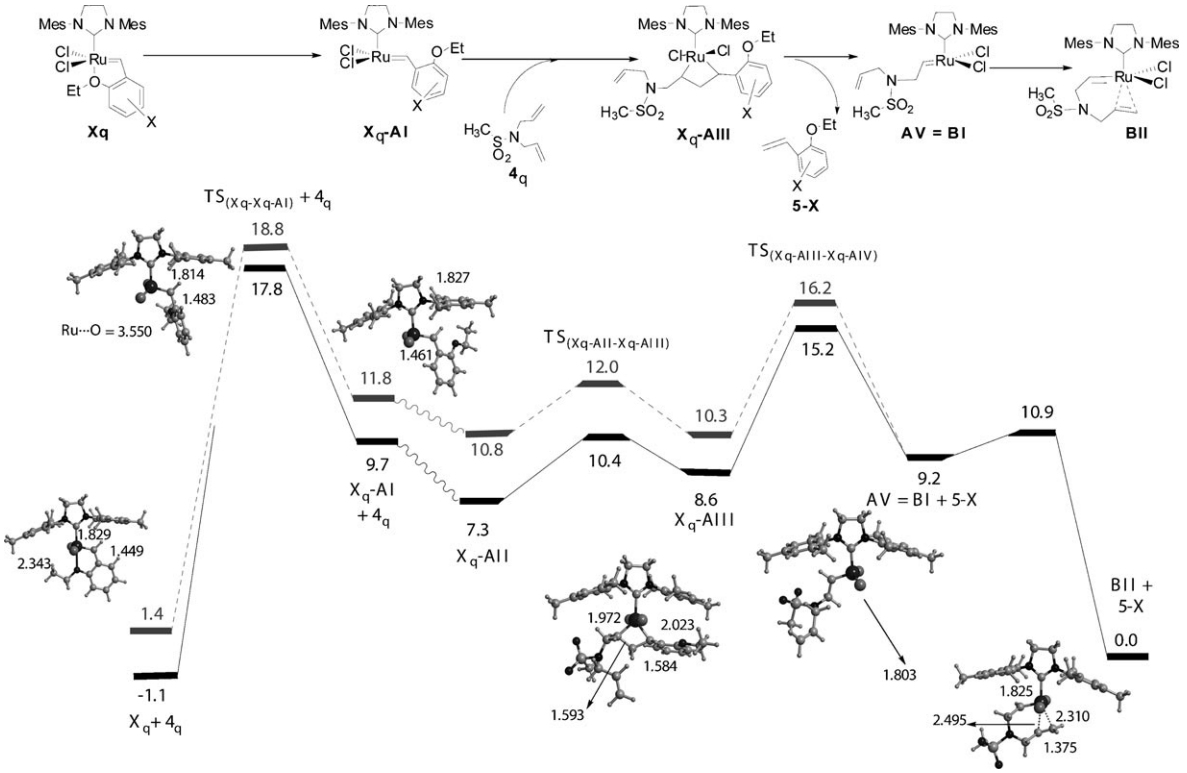

Figure 1. Energy profile (based on $E+\Delta G_{solv}$ in kcal mol^{-1}) for **BII** catalyst generation (Scheme 5) from cross-metathesis between precatalyst $\mathbf{H_q}$ (black solid curve) or $\mathbf{NO_2(4)_q}$ (gray dotted curve) and $\mathbf{4_q}$. Some selected optimized structures (distances in Å) have been added. All relative energies are with respect to the **BII**+**5-X** propagating carbene. Absolute energy values can be found in the Supporting Information.

(1.827 Å), and the C1–C2 distance is also longer (1.483 vs. 1.449 in $\mathbf{H_q}$ and 1.461 Å $\mathbf{H_q}$-**AI**). This is consistent with a partial loss of the C1–C2 π-bond character. As a result of these electronic changes, the process is endoenergetic by 10.8 kcal mol^{-1} and the energy barrier is 18.9 kcal mol^{-1}.

Coordination of $\mathbf{4_q}$ leads to an olefin complex ($\mathbf{H_q}$-**AII**) in which the carbene ligand has rotated 90°. Although this is not the preferred orientation from an electronic point of view, carbene rotation is easy and this reorganization minimizes the steric repulsion between the carbene moiety and the incoming olefin. Note that the equivalent $\mathbf{H_q}$-**AI** structure with the carbene rotated 90° is not a minimum on the potential-energy surface but a rotational transition state that lies 6.5 kcal mol^{-1} above $\mathbf{H_q}$-**AI**. This energy cost is recovered by the olefin coordination, since the resulting $\mathbf{H_q}$-**AII** structure is 2.4 kcal mol^{-1} more stable than $\mathbf{H_q}$-**AI**. The olefin complex $\mathbf{H_q}$-**AII** can easily evolve, through a 3.1 kcal mol^{-1} energy barrier, to the metallacycle intermediate ($\mathbf{H_q}$-**AIII**), which is 1.3 kcal mol^{-1} above $\mathbf{H_q}$-**AII**. The metallacyclobutane has a trigonal bipyramidal structure (TBP), with the two chloride ligands being apical, whereas the NHC carbene and the metallacyclobutane moiety are in the equatorial plane. As already reported for other Ru-based catalysts, the metallacyclobutane is flat and presents a considerably short M···C_β distance.[59] It is worth mentioning that we have not been able to locate a square-based pyramidal (SBP) metallacyclobutane intermediate as a minimum on the potential-energy surface. These species have been identified in Schrock-type catalysis[60] and have been suggested to be a resting state that may be the origin of several deactivation pathways.[27,61] The nonexistence of the SBP metallacycle intermediate has an electronic origin and can be explained using the molecular orbital treatment for pentacoordinated transition-metal complexes that was developed by Rossi and Hoffmann in 1975[62] (see the Supporting Information for details).

Metallacyclobutane opening has an energy barrier of 6.6 kcal mol^{-1} and it evolves spontaneously to **BI** (also called **AV**). The reaction energy is +0.6 kcal mol^{-1}. The **BI** species does not have the Hoveyda ligand and thus it models one of the propagating carbenes in solution. It largely resembles $\mathbf{H_q}$-**AI**, with a seesaw structure and coplanar Ru=C and NHC moieties. Remarkably, the Ru=C bond length in **BI** is 1.803 Å (Figure 2), which is considerably shorter than that in $\mathbf{H_q}$-**AI** (1.827 Å, Figure 1).

Once **BI** is formed, the system enters the real catalytic cycle (Scheme 5B, Figure 2, and Figure S3 in the Supporting Information). All the intermediates and transition states are similar to those found between $\mathbf{H_q}$-**AI** and **BI**. Thus, no further geometrical details will be presented. The most significant difference between the two processes A and B (Scheme 5) is that the metal vacant site at **BI** is not saturated by an incoming olefin, which will lead to a cross-metathesis process, but it is occupied by the second C=C double

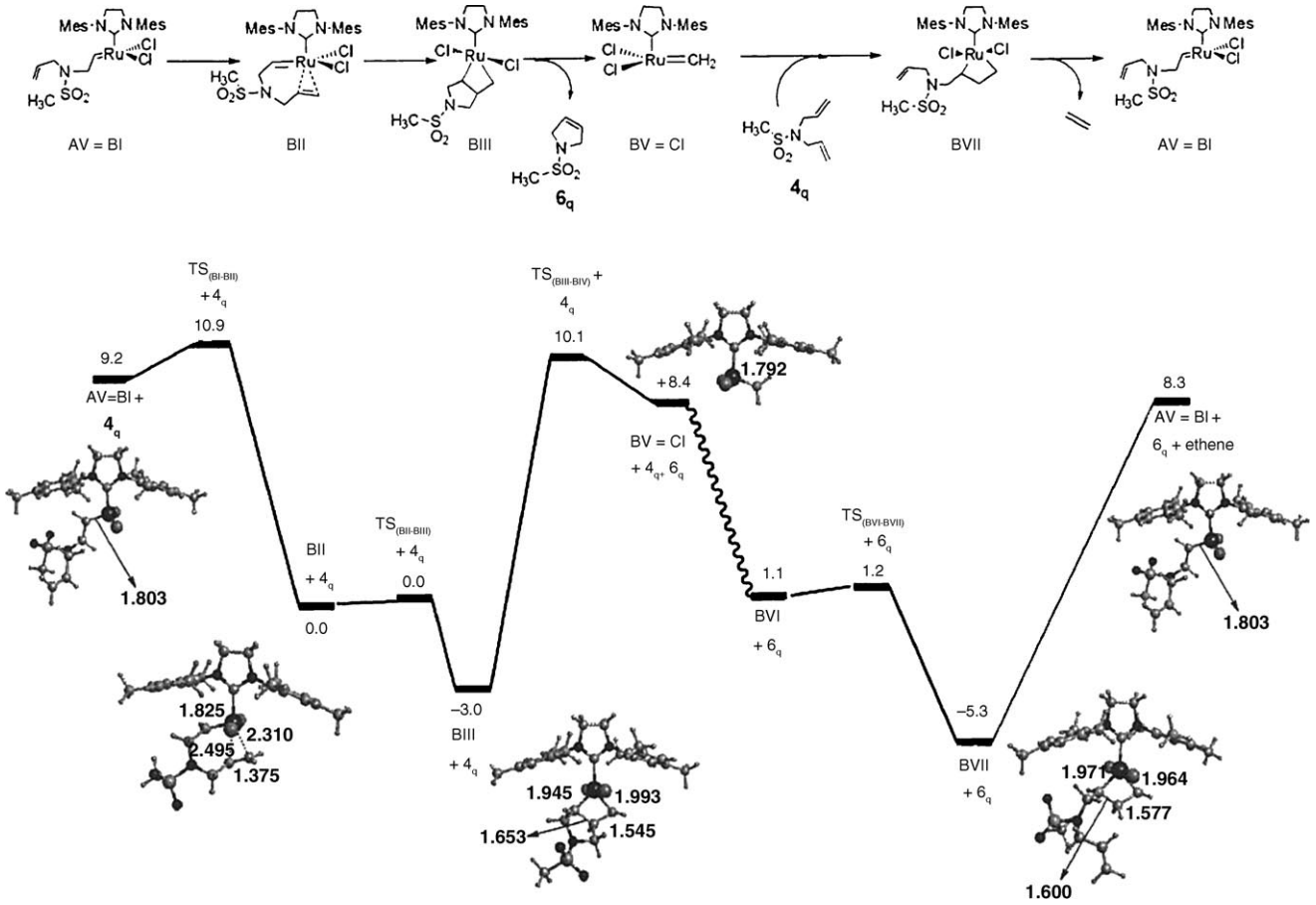

Figure 2. Energy profile (based on $E+\Delta G_{solv}$ in kcal mol^{-1}) for the catalytic cycle of ring-closing metathesis ($\mathbf{4_q}\rightarrow\mathbf{6_q}$+ethene) (Scheme 5). Some selected optimized structures (distances in Å) have been added. All relative energies are with respect to the **BII**+**5-X** propagating carbene. Absolute energy values can be found in the Supporting Information.

bond of the sulfonamide ($\mathbf{4_q}$). This C=C coordination produces a considerable geometry reorganization of the carbene ligand, but since this rearrangement mainly implies C–C simple bonds and the rotation of the Ru=C carbene bond (**BII**), the associated energy barrier is low (1.7 kcal mol^{-1}). Overall, cycle B has relatively low energy barriers. The highest energy barriers are associated with the two metallacyclobutane opening processes, **BIII** to **BV** and **BVII** to **BI**, similarly to what is observed in process A, if one does not consider the alkoxy ligand dissociation. Thus, the ring opening appears to be the key step of the olefin metathesis process itself (Chauvin's mechanism). The energy barriers for **BIII** to **BV** and **BVII** to **BI** processes are 13.1 and 13.6 kcal mol^{-1}, respectively. It should be mentioned that in most of the cases computed here and at the level of theory used, the hypothetical olefin complex that could be formed after cycloreversion is not a minimum of the potential-energy surface; olefin dissociation occurs spontaneously. According to the analysis included in Table S2 of the Supporting Information, the alkene complex stability with respect to separate reactants depends on two main factors: 1) the steric repulsion between the incoming olefin and the ligands of the metal complex, and 2) the entropic cost (included partially in the $E+\Delta G_{solv}$ values) associated with the alkene formation. Regarding the first factor, it is observed that olefins with small substituents get closer to the metal center (shorter Ru···$C_{(alkene)}$ distance), and therefore the Ru–olefin interaction is higher. Nevertheless, if the olefin is small enough and the alkylidene complex has no steric hindrance, the cycloaddition may be so easy that the transition state does not exist at the present level of theory and cycloaddition occurs without forming the alkene complex. This is the case for **BVIII**, for which we have not been able to find any transition-state structure and any complex with the coordinated ethene, although detailed exploration has revealed a very flat region between 7 and 8 kcal mol^{-1} lower in energy than **BI**. Regarding the entropic contribution, this factor only applies to the **BII** intermediate in the present reaction. In that case, the potential-energy difference between **BII** and **BI** reveals that **BII** is not one of the most stable alkene complexes with respect to separate species as should be expected from the size and hindrance of their substituents. In fact, the high stability of this complex arises from ΔG_{solv} values since the process is intramolecular and there is less entropy loss.

Finally, if the boomerang effect applies, catalyst precursor regeneration may occur through two pathways. On the one

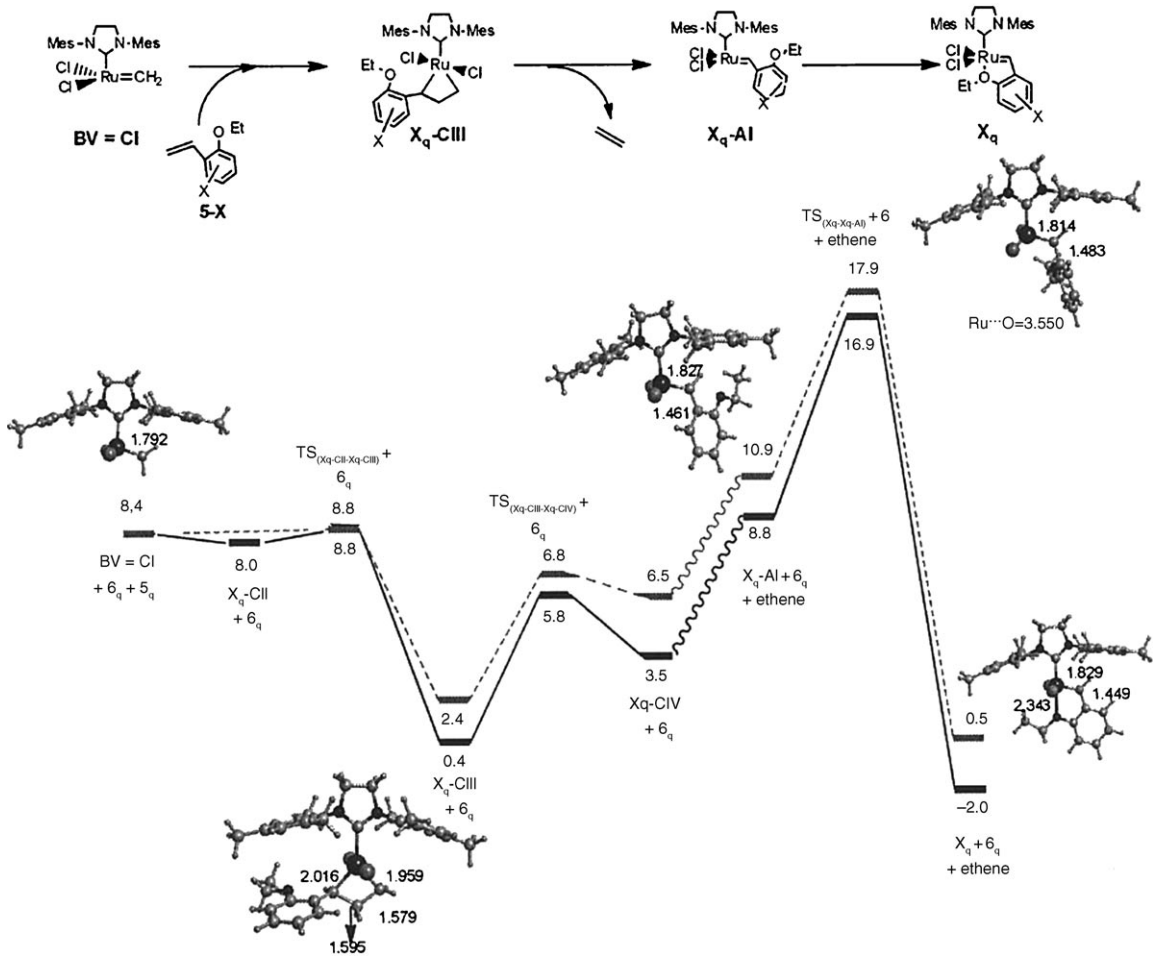

Figure 3. Energy profile (based on $E+\Delta G_{solv}$ in kcal mol^{-1}) for the precatalyst regeneration (Scheme 5) by means of cross-metathesis of **5-X** with **CI** (X = **H** in the black solid curve and **NO_2(4)** in the gray dotted one). Some selected optimized structures (distances in Å) have been added. All relative energies are with respect to the **BII**+**5-X** propagating carbene. Absolute energy values can be found in the Supporting Information.

hand, the styrene **5-H** can react with **BI** and thus proceed through the inverse reaction of that described in path A (Scheme 5). On the other hand, the **5-H** olefin can react with **CI**, thereby undergoing the process described in path C of Scheme 5. The most significant intermediates and transition states involved in path C as well as the associated energy profile are represented in Figure 3. All other optimized structures are shown in Figure S4 in the Supporting Information. The formation of a species that contains the Hoveyda ligand interacting covalently with the metal center (**H_q-AIII**, **H_q-CIII**, and **H_q-AI**) requires low energy barriers (less than 9 kcal mol^{-1}), and the only significant energy barrier is associated with the formation of **H_q**. Nevertheless, the **H_q** precursor is the only carbene that has similar relative energies to the most stable carbene in solution, **BII**, and thus its formation is required to form a species stable enough to be recovered. All other species (**CI**, **H_q-AI**) are significantly higher in energy than **BII** and can easily evolve to it (low energy barriers). Overall, formation of **H_q**, either through path A or C, suggests a crossing over of the high energy barrier associated with alkoxy coordination. The transition state is 8.1 kcal mol^{-1} higher in energy than **H_q-AI**, and the apparent barrier (barrier with respect to **BII**) is 17.8 kcal mol^{-1} through process A and 16.9 kcal mol^{-1} through process C, the difference between the two values being the computed ring-closing diene metathesis thermodynamics (**4_q**→**6_q**+ ethene).

Scheme 6 summarizes, in a simplistic manner, the studied reactions including their thermodynamics (ΔE) and the energy span between the lowest minima and the highest transition state ($\Delta E^{\neq}$). The highest energy barrier is associated with the chelating Hoveyda ligand dissociation and thus the catalytic activity seems to be mainly controlled by the ability of the precursor to generate the active carbene. Once the alkoxy ligand is dissociated, all the remaining energy barriers are low. The barriers are so low that one can assume that the equilibrium is reached easily after dissociation. Nevertheless, since the species of the catalytic cycle are generally more stable than those that contain the Hoveyda ligand—the only exception being **H_q**, the formation of which requires a relatively high energy barrier—one can conclude that **BI** and **CI** would react faster with the more abundant

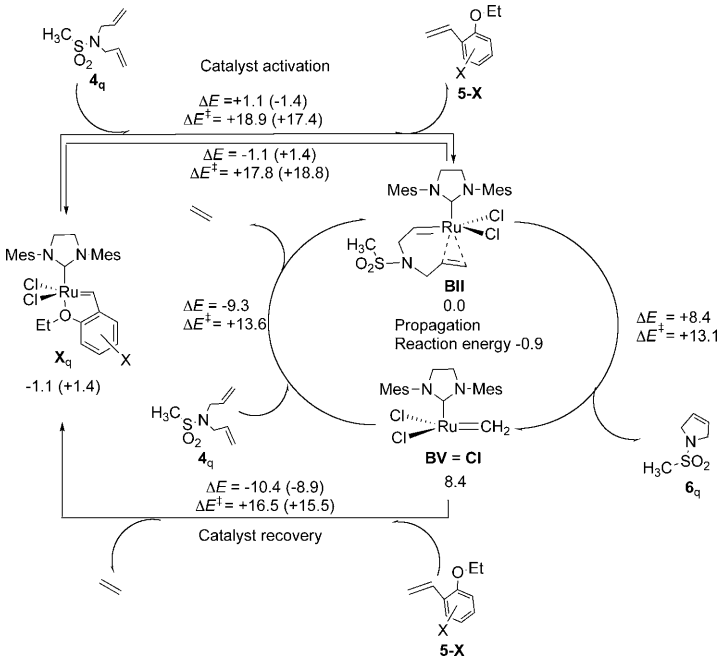

Scheme 6. Simplified representation of all studied reactions including reaction thermodynamics (ΔE) and energy span between the lowest-energy intermediate and the highest transition state ($\Delta E^{\neq}$) for $\mathbf{H_q}$ in black and $\mathbf{NO_2(4)_q}$ within parentheses in gray. All energies are in kcal mol^{-1}.

diene molecule ($\mathbf{4_q}$) than with the Hoveyda ligand **5-H**. In fact, $\mathbf{H_q}$ regeneration by the reaction of the propagating carbenes **BI** or **CI** with **5-H** would be thermodynamically possible but it would almost only take place after consumption of the reactants, if the catalyst has not been yet deactivated.

The addition of a nitro group into the chelating Hoveyda ligand in the *para* position to the leaving alkoxy group does not modify the global mechanism and, in particular, all intermediates present equivalent geometries (Figures S5 and S6 in the Supporting Information). Thus, in the following discussion we will only mention those subtle variations that we consider significant to the analysis.

Regarding the catalyst generation process (path A), it is worth mentioning that $\mathbf{NO_2(4)_q}$ presents a longer Ru···O distance (2.359 Å) than that optimized for $\mathbf{H_q}$ (2.343 Å). Moreover, it presents slightly shorter Ru=C (1.825 vs. 1.829 Å) and slightly longer C1−C2 (1.453 vs. 1.449 Å) bond lengths (Scheme 2, Figure 1, and Figures S1 and S5 in the Supporting Information). These trends are maintained in the $\mathbf{TS_{(NO_2(4)_q\text{-}to\text{-}NO_2(4)_q\text{-}AI)}}$ and $\mathbf{NO_2(4)_q}$-**AI** structures and are associated with a lower energy barrier for the alkoxy dissociation in $\mathbf{NO_2(4)_q}$ (17.4 vs. 18.9 kcal mol^{-1}). In addition, once $\mathbf{NO_2(4)_q}$-**AI** is formed, all energy barriers that lead to **BI** are low. The highest one corresponds to the metallacyclobutane ring opening of $\mathbf{NO_2(4)_q}$-**AIII** and is only 5.9 kcal mol^{-1}. Catalyst precursor regeneration (path C in Figure S6) also requires the alkoxy coordination process from $\mathbf{NO_2(4)_q}$-**AI** to $\mathbf{NO_2(4)_q}$, since $\mathbf{NO_2(4)_q}$ is the only species that has comparable energy to **BII**. This suggests a crossing over of the alkoxy coordination transition-state structure ($\mathbf{TS_{(NO_2(4)_q\text{-}to\text{-}NO_2(4)_q\text{-}AI)}}$), the energy barrier of which is 18.8 or 17.9 kcal mol^{-1} above the most stable carbene in solution (**BII**), depending on whether it proceeds along path A or C, respectively.

The experimental evidence shows that molecular $\mathbf{NO_2(4)_M}$ and heterogenized $\mathbf{NO_2(4)}$ precatalysts present higher activities (higher conversions per time unit) than the analogous molecular and heterogenized ($\mathbf{H_M}$ and **H**) species. Nevertheless, **H** and $\mathbf{H_M}$ are recovered in a larger amount than $\mathbf{NO_2(4)}$ or $\mathbf{NO_2(4)_M}$ after the catalytic ring-closing diene metathesis cycle.[20,22] Although the computed energy barriers and stabilities for $\mathbf{H_q}$ and $\mathbf{NO_2(4)_q}$ differ only marginally, present calculations are able to explain the experimental trends. That is, results suggest that the activity is determined by the ability of the precursor to generate the active carbene either considering a kinetic factor (alkoxy dissociation is easier for $\mathbf{NO_2(4)_q}$ than for $\mathbf{H_q}$ ($\Delta E^{\neq} = 17.4$ vs. 18.9 kcal mol^{-1})) or a thermodynamic criterion (formation of the active species is only favorable for $\mathbf{NO_2(4)_q}$ ($\Delta E = -1.4$ vs. $+1.1$ kcal mol^{-1})). In addition, they predict that the recovery of the precatalyst is determined either by the amount of precatalyst that has not reacted or by a more efficient release–return mechanism (the boomerang effect).The former correlates with the alkoxy-dissociation energy ($\mathbf{H_q} > \mathbf{NO_2(4)_q}$) and implies that the equilibrium is not reached. The latter depends on the relative stabilities of the precatalyst and the active carbenes in solution and implies that thermodynamical equilibrium is reached. That is, besides any potential deactivation of the Ru-based species or the Hoveyda ligand, if the system is allowed to evolve until thermodynamic equilibrium, the amount of precatalyst would depend on the relative stabilities between the precursor and the active carbene complexes (Scheme 6). Here, the methylidene complex (**CI**), which is formed during many olefin metathesis processes, is considerably higher in energy than either **BII** or the precatalyst and thus its abundance in a hypothetical equilibrium would be negligible. In contrast, **BII**, which is specific to the studied reaction, and the precatalyst ($\mathbf{X_q}$) are much closer in energy and thus their relative stabilities are expected to be the key factor for evaluating if the boomerang effect (release–return mechanism) is possible or not. The relative energies between $\mathbf{H_q}$ and $\mathbf{NO_2(4)_q}$ and **BII** are close to zero (Figure 1), and this seems to suggest that catalyst recovery is possible, which is in agreement with isotopic labeling experiments performed by Hoveyda et al.[18] and Grela et al.[56] However, calculations indicate that the return of $\mathbf{NO_2(4)_q}$ catalyst would be less efficient than that of $\mathbf{H_q}$, which is in agreement with the loss of activity in diene metathesis after several runs of $\mathbf{NO_2(4)_{SiO_2}}$ and the generally observed lower recovery of $\mathbf{NO_2(4)_H}$ after product–catalyst separation by chromatography.[20,22]

At this point, it is worth mentioning that the present modeling strategy is not sufficient to distinguish between kinetic or thermodynamic control. Therefore, it is not possible to identify whether the degree of catalyst recovery comes from nonreacted precatalyst or from the return of the active spe-

cies when the reaction is complete. One would expect the first possibility if the energy barrier associated with alkoxy dissociation is high enough to avoid reaching the equilibrium during reaction times. The boomerang effect would only occur if equilibrium is reached, and this implies a relatively low alkoxy-dissociation energy barrier. Unfortunately, the alkoxy-dissociation energies computed here range between 17 and 25 kcal mol^{-1} depending on the system and the level of calculation (Table S1 in the Supporting Information). Thus, although the two levels of theory used here are accurate enough to correctly reproduce trends, it is more difficult to determine absolute values; the B3LYP ones suggest that the equilibrium could be reached during the reaction time (18–20 kcal mol^{-1}), whereas the M06L or M06X ones suggest that most of the precatalyst would not dissociate during the reaction time (23–25 kcal mol^{-1}).

For a further understanding of how the activity of these complexes is affected by the presence of substituents in the phenyl ring, we have performed calculations that consider both electron-withdrawing and electron-donor substituents at different positions of the phenyl ring (Scheme 2). Compounds $\mathbf{H_q}$, $\mathbf{NO_2(4)_q}$, $\mathbf{NO_2(5)_q}$, $\mathbf{OMe(4)_q}$, and $\mathbf{OMe(5)_q}$ are models of the existing $\mathbf{H_M}$, $\mathbf{NO_2(4)_M}$, $\mathbf{NO_2(5)_M}$, $\mathbf{O}i\mathbf{Pr(4)_M}$, and $\mathbf{O}i\mathbf{Pr(5)_M}$ ones, the catalytic rates of which generally seem to vary in the order $\mathbf{NO_2(4)_M} \approx \mathbf{NO_2(5)_M} > \mathbf{H_M} > \mathbf{O}i\mathbf{Pr(5)_M} > \mathbf{O}i\mathbf{Pr(4)_M}$.[22,23] Since the activity is determined by the ability of the precursor to generate the active species (alkoxy decoordination and/or relative energies between the precursor and the propagating carbene) and the catalyst recovery depends on the same two factors, our efforts in the following section are only focused on these two parameters.

Effect of electron-donor and electron-withdrawing substituents at the chelating Hoveyda ligand on the activity and catalyst recovery: Figure 4 and Figure S7 in the Supporting Information show the optimized structures of $\mathbf{X_q}$ catalyst precursors and $\mathbf{TS_{Xq\text{-}to\text{-}Xq\text{-}AI}}$, respectively. Table 1 reports the alkoxy-dissociation energy barriers and the relative energies of $\mathbf{X_q}+\mathbf{4_q}$ with respect to the **BII+5-X** asymptote (see Schemes 2, 4, and 5 for species definition). All $\mathbf{X_q}$ complexes present equivalent structures with the same distorted SBP coordination around the metal center and the same Ru=C and NHC relative orientation. On going into detail, one can observe that phenyl ring substitution produces significant variations on the Ru···O, Ru=C1, and C1−C2 distances (Scheme 1). For instance, it is observed that the higher the electron-donor capacity of the substituent at C4 (Scheme 1), the shorter the Ru···O distance is; a clear example of this is the shortening of the Ru···O distance on going from $\mathbf{H_q}$ (2.343 Å) to $\mathbf{OMe(4)_q}$ (2.331 Å). In contrast, the opposite effect is observed with the substituents at C5, that is, the strongest electron-donor substituent in C5 leads to the largest Ru···O bond. For instance, the $\mathbf{OMe(5)_q}$ (2.360 Å) catalyst presents a considerably longer distance than $\mathbf{H_q}$ (2.343 Å). These variations can be rationalized by considering that the Ru···O distance arises from the interaction between a Lewis acidic metal center and an alkoxy Lewis base. Therefore, the interaction will be favored when increasing the electron density in the alkoxy group and decreasing that of the metal. Since benzene substituents mainly tune the *ortho* and *para* positions, one can assume in

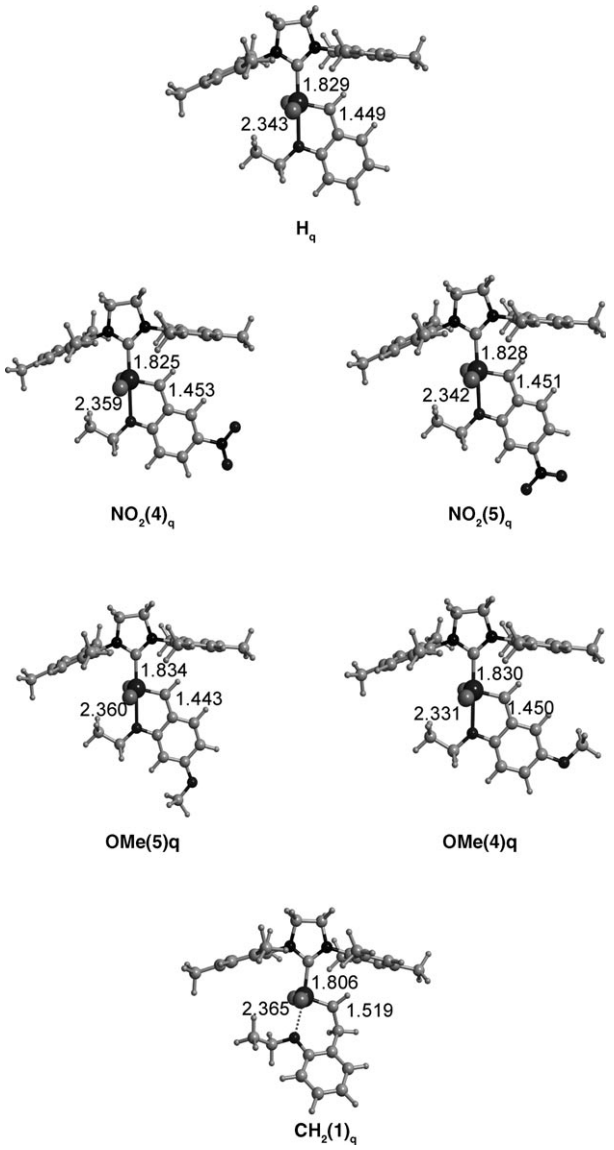

Figure 4. Precatalyst optimized geometries (distances in Å)

Table 1. Alkoxy-dissociation energy barrier ($\Delta E^{\neq}$ in kcal mol^{-1}) and relative energies of the $\mathbf{4_q}+\mathbf{X_q}$[a] precatalyst with respect to the **BII+5-X**[b] asymptote.

Precatalyst[a]	$\Delta E^{\neq}$	$\mathbf{X_q}$
$\mathbf{H_q}$	18.9	−1.1
$\mathbf{NO_2(4)_q}$	17.4	+1.4
$\mathbf{NO_2(5)_q}$	17.3	+1.2
$\mathbf{OMe(4)_q}$	19.8	−1.1
$\mathbf{OMe(5)_q}$	19.0	−1.4
$\mathbf{CH_2(1)_q}$	6.6	+7.5

[a] See Schemes 2 and 7 for a definition of the precatalysts. [b] See Schemes 4 and 5 for a definition of the species.

a first approximation that the substituent at C4 mainly tunes the electron density on the O atom and the substituent at C5 mainly tunes that of the carbene, thereby indirectly modifying that of the metal center. Therefore, the addition of an electron-donor substituent in C5 increases the electron density of the carbene and consequently that of the metal, thus disfavoring the Ru···O interaction, whereas alkoxy groups in C4 would increase the electron density of the O atom, thus strengthening the Ru···O interaction.

As mentioned before, the presence of these substituents in the phenyl ring does not only alter the Ru···O interaction. It also varies the Ru=C1 and C1−C2 bonds. In particular, the more of an electron donor the phenyl substituent, the longer the Ru=C1 distance and the shorter the C1−C2 bond is. This is particularly important for substituents at C5 (*para* to the Ru=C1 bond). As an example, the Ru=C1 distance elongates from 1.828 to 1.834 Å on going from $\mathbf{NO_2(5)_q}$ to $\mathbf{OMe(5)_q}$ and the opposite effect is observed for C1−C2, which shortens from 1.451 to 1.443 Å. This may be explained by the delocalization of the π system. That is, since the carbene and the phenyl are coplanar, they are conjugated and the C1−C2 bond has some double-bond character. The π character of the C1−C2 bond increases with the presence of electron-donor groups at C5, thereby leading to shorter C1−C2 distances. Variations of the π system also affect the Ru=C1 bond that becomes longer with the presence of donor groups.

As in previous cases, all transition-state structures $\mathbf{TS_{Xq\text{-}Xq\text{-}AI}}$ have a phenyl ring that has almost rotated 90° along the C1−C2 bond (Figure S7 in the Supporting Information); they do not present an Ru···O interaction, as evidenced by the long Ru···O distance, and their C1−C2 bond length is elongated by about 0.03 Å with respect to that of the minimum. That is, at the transition state, the C1−C2 bond is closer to that of the single bond than in the catalyst precursor, thereby suggesting a decrease in the π delocalization since now the carbene and the phenyl π systems are almost perpendicular and there is not much overlap.

The computed energy barriers for alkoxy dissociation (Table 1) range between 17.3 and 19.8 kcal mol^{-1}. It is important to note that although these energy barriers differ only marginally, they follow the experimentally observed catalytic activities for these compounds $\mathbf{NO_2(4)_H}$, $\mathbf{NO_2(5)_H} > \mathbf{H_H} > \mathbf{O}i\mathbf{Pr(4)_H}$, $\mathbf{O}i\mathbf{Pr(5)_H}$. Interestingly, the relative energies between $\mathbf{X_q+4_q}$ and **BII+5-X** also correlate reasonably well with the experimentally observed activities. Overall, calculations are accurate enough to reproduce the main trends that have traditionally been associated with the Ru···O interaction.[22–24] Nevertheless, the present calculations show that there is no direct relationship between the energy barrier and the Ru···O interaction strength. This is clearly exemplified when comparing $\mathbf{OMe(5)_q}$ to $\mathbf{NO_2(5)_q}$. The former presents a larger Ru···O distance than the latter (2.360 vs. 2.342 Å), but $\mathbf{O}i\mathbf{Pr(5)_H}$ is less active than $\mathbf{NO_2(5)_H}$ and, in fact, $\mathbf{OMe(5)_q}$ presents one of the highest computed energy barriers and it is more stable than the propagating species, whereas $\mathbf{NO_2(5)_q}$ presents the lowest energy barrier and it is less stable than **BII+5-X**. That is, although the Ru···O distance may tune the catalytic activity, results show that the experimentally observed catalytic efficiencies correlate better with the C1−C2 bond length, that is, its double-bond character. This double-bond character is indicative of the π-electron density delocalization, which is almost completely lost during alkoxy dissociation. In this way, the energy barrier ($\mathbf{NO_2(5)_q} < \mathbf{NO_2(4)_q} < \mathbf{H_q} < \mathbf{OMe(5)_q} < \mathbf{OMe(4)_q}$), the relative energies between precursor and propagating species ($\mathbf{NO_2(4)_q} < \mathbf{NO_2(5)_q} < \mathbf{H_q} = \mathbf{OMe(4)_q} < \mathbf{OMe(5)_q}$), and the C1−C2 distance ($\mathbf{NO_2(4)_q} > \mathbf{NO_2(5)_q} > \mathbf{OMe(4)_q} > \mathbf{H_q} > \mathbf{OMe(5)_q}$) vary very similarly. These results go in the same direction as Grela's and Barbasiewicz's experiments[62] on naphthalene-based analogues of the Hoveyda–Grubbs metathesis catalysts. In their study, they performed a structural and spectroscopic analysis of these complexes that revealed that the ruthenafurane ring possesses some aromatic character, which would inhibit catalyst activity. More interestingly, on the basis of this aromatic character of the ruthenafurane ring, the authors proposed that the nitro-substituted catalyst ($\mathbf{NO_2(4)_H}$) shows decreased aromaticity (and enhanced activity) due to the contribution of a quinonoid-type structure.[63]

The relative energies of $\mathbf{X_q+4_q}$ with respect to the **BII+5-X** asymptote are also summarized in Table 1 and they range from −1.4 to +1.4 kcal mol^{-1}, thereby suggesting that, at least from a thermodynamic point of view, the boomerang effect is possible but is sensitive to the phenyl substituents. The computed trend—either taking alkoxy-dissociation energy barriers or the relative stabilities between the precursor and the active carbene as criteria—are consistent with the experimental evidence: nitro-substituted compounds generally exhibit a lower recovery than the corresponding nonsubstituted ones.[20,22] More interestingly, calculations show that there is no relationship between recovery and the Ru···O interaction. For instance, $\mathbf{NO_2(5)_q}$ presents a short Ru···O distance but the alkoxy-dissociation energy barrier is low and its stability with respect to **BII** slightly disfavored. On the contrary, $\mathbf{OMe(5)_q}$ presents a long Ru···O distance but a high alkoxy-dissociation energy and higher stability of the precursor than any of the carbene species in the real catalytic cycle. Overall, π delocalization also seems to be the key factor in determining catalyst recovery, since alkoxy dissociation correlates with the C1−C2 bond length and the stability of the precursor correlates well with the Ru=C1 distances. That is, the shorter the Ru=C1 distance, the longer the C1−C2 bond and the lower the catalyst recovery is predicted to be.

To confirm the present conclusions, we considered an additional complex, $\mathbf{CH_2(1)_q}$, which has no conjugation between the phenyl and the carbene (Scheme 7 and Figure 4). Although this complex has never been synthesized and its synthesis may not be trivial, $\mathbf{CH_2(1)_q}$

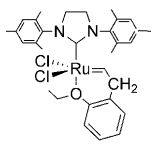

$\mathbf{CH_2(1)_q}$

Scheme 7.

has been designed to verify the influence of the π delocalization in the alkoxy-dissociation barrier.

The addition of a sixth carbon in the original five-membered ring defined by Ru, C1, C2, C7, and O produces important geometrical variations. The phenyl ring loses its coplanarity with the NHC carbene ligand and the Ru···O distance is 0.022 Å larger than that of $\mathbf{H_q}$. These two effects suggest a weaker interaction between the alkoxy chelating ligand and the Ru metal center in $\mathbf{CH_2(1)_q}$. Nevertheless, the most remarkable geometrical variations are associated with the carbene fragment. As expected, the C1−C_β bond length (1.519 Å) is close to that of a single C−C bond. Moreover, the Ru=C bond is much shorter (Ru=C1 = 1.806 Å). Altogether, the large C1−C_β bond length, the weaker Ru···O interaction, and the stronger Ru=C bond lead to an alkoxy-dissociation barrier that is impressively lower (more than 10 kcal mol^{-1}) than the previously reported ones, but also the stability of the precursor is negligible with respect to **BII**, thereby indicating that $\mathbf{CH_2(1)}$ would not be recovered even if the system were allowed to evolve until equilibrium and no deactivation were to take place (see Table 1). Both the low barrier and the low stability of $\mathbf{CH_2(1)_q}$ can not only be associated with the weakening of the Ru···O interaction, but they mainly seem to arise from the loss of carbene–phenyl π delocalization, thereby confirming its dramatic influence.

Conclusion

The current work presents an exhaustive theoretical mechanistic study on the diene ring-closing metathesis catalyzed by Ru-based Grubbs–Hoveyda carbenes. The full catalytic cycle (catalyst formation, propagation, and precatalyst regeneration) as proposed in the literature[18,56,57] is considered. Results show that all energy barriers associated with the metathesis process itself (Chauvin's mechanism) are low (less than 14 kcal mol^{-1}) and, in fact, the only relatively high energy barrier is the initial alkoxy dissociation (values ranging between 17 and 25 kcal mol^{-1}, depending on the precatalyst nature and level of calculation). Since the propagating cycle is equal for all systems, differences in activity arise from the ability of the precursor to generate the active species. In fact, the $\mathbf{NO_2(4)_q}$ complex generates the propagating species easily either considering a kinetic (lower barrier height for the most demanding alkoxy dissociation) or thermodynamic criterion (relative stabilities of $\mathbf{H_q}$ and $\mathbf{NO_2(4)_q}$ compared to the propagating **BII** species).

The alkoxy dissociation proceeds through the C1−C2 bond rotation (Scheme 1), which leads to a transition-state structure in which the phenyl ring of the Hoveyda ligand and the Ru=C bond are almost perpendicular. This orientation prevents the π delocalization, which exists in the initial precatalyst between the phenyl and the carbene, from occurring at the transition state, which turns out to be the key factor controlling the alkoxy-dissociation energy barrier. Therefore, the Ru···O interaction strength does not correlate with the alkoxy-dissociation energy barriers as previously suggested. Instead, it is observed that the higher the π delocalization between the phenyl and the Ru=C bond in the precatalyst, the higher the energy barrier and thus the lower the catalytic activity.

The loss of catalytic activity after several runs is also related to the π delocalization either if the amount of recovered catalyst after reaction comes from the nonreacted precatalyst or from the so-called boomerang effect. For the former situation, the higher the alkoxy-dissociation energy barrier, the higher the amount of recovered catalyst would be. For the latter situation, the recovery depends on the relative energies between the precatalyst and the active carbenes: π delocalization increases the stability of the initial precatalyst and thus at thermal equilibrium its abundance would be higher.

In summary, the present calculations show that the Ru···O interaction is not the determining factor on the catalytic activity and catalyst recovery. They rather depend on the π delocalization between the phenyl and the carbene in the precatalyst. Therefore, future developments in Grubbs–Hoveyda-type catalysts should be based on the influence of phenyl substituents on the π-electron density in the phenyl-ring fragment, with the subsequent effect on the metalloaromaticity of the ruthenafurane ring.

Acknowledgements

We acknowledge financial support from MEC/MICINN of Spain (projects CTQ2006-04204/BQU and CTQ2008-06381/BQU), Consolider Ingenio 2010 (CSD2007-00006), Generalitat de Catalunya (projects SGR2009-01441 and SGR2009-638). X.S.M. also thanks the Spanish MEC/MICINN for the Ramón y Cajal fellowship.

[1] R. H. Grubbs, *Angew. Chem.* **2006**, *118*, 3845–3850; *Angew. Chem. Int. Ed.* **2006**, *45*, 3760–3765.
[2] R. H. Grubbs, S. Chang, *Tetrahedron* **1998**, *54*, 4413–4450.
[3] M. R. Buchmeiser, *Chem. Rev.* **2000**, *100*, 1565–1604; C. Copéret, *Dalton Trans.* **2007**, 5498–5504; J. C. Mol, *J. Mol. Catal. A* **2004**, *213*, 39–45; A. Fürstner, *Angew. Chem.* **2000**, *112*, 3140–3172; *Angew. Chem. Int. Ed.* **2000**, *39*, 3012–3043; D. Astruc, *New J. Chem.* **2005**, *29*, 42–56.
[4] R. R. Schrock, *Angew. Chem.* **2006**, *118*, 3832–3844; *Angew. Chem. Int. Ed.* **2006**, *45*, 3748–3759; R. R. Schrock, A. H. Hoveyda, *Angew. Chem.* **2003**, *115*, 4740–4782; *Angew. Chem. Int. Ed.* **2003**, *42*, 4592–4633.
[5] C. Copéret, J. M. Basset, *Adv. Synth. Catal.* **2007**, *349*, 78–92.
[6] T. M. Trnka, R. H. Grubbs, *Acc. Chem. Res.* **2001**, *34*, 18–29.
[7] C. Pariya, K. N. Jayaprakash, A. Sarkar, *Coord. Chem. Rev.* **1998**, *168*, 1–48.
[8] D. Burtscher, K. Grela, *Angew. Chem.* **2009**, *121*, 450–462; *Angew. Chem. Int. Ed.* **2009**, *48*, 442–454.
[9] C. Copéret, M. Chabanas, R. P. Saint-Arroman, J. M. Basset, *Angew. Chem.* **2003**, *115*, 164–191; *Angew. Chem. Int. Ed.* **2003**, *42*, 156–181.
[10] R. R. Schrock, *Chem. Rev.* **2002**, *102*, 145–179.
[11] S. T. Nguyen, L. K. Johnson, R. H. Grubbs, J. W. Ziller, *J. Am. Chem. Soc.* **1992**, *114*, 3974–3975.
[12] M. Scholl, S. Ding, C. W. Lee, R. H. Grubbs, *Org. Lett.* **1999**, *1*, 953–956; M. Scholl, T. M. Trnka, J. P. Morgan, R. H. Grubbs, *Tetrahedron*

Lett. **1999**, *40*, 2247–2250; L. Ackermann, A. Fürstner, T. Weskamp, F. J. Kohl, W. A. Herrmann, *Tetrahedron Lett.* **1999**, *40*, 4787–4790.
[13] J. S. Kingsbury, J. P. A. Harrity, P. J. Bonitatebus, A. H. Hoveyda, *J. Am. Chem. Soc.* **1999**, *121*, 791–799.
[14] S. B. Garber, J. S. Kingsbury, B. L. Gray, A. H. Hoveyda, *J. Am. Chem. Soc.* **2000**, *122*, 8168–8179.
[15] M. S. Sanford, J. A. Love, R. H. Grubbs, *J. Am. Chem. Soc.* **2001**, *123*, 6543–6554; K. Getty, M. U. Delgado-Jaime, P. Kennepohl, *J. Am. Chem. Soc.* **2007**, *129*, 15774–15776.
[16] S. Torker, D. Merki, P. Chen, *J. Am. Chem. Soc.* **2008**, *130*, 4808–4814.
[17] M. Ahmed, A. G. M. Barrett, D. C. Braddock, S. M. Cramp, P. A. Procopiou, *Tetrahedron Lett.* **1999**, *40*, 8657–8662; S. T. Nguyen, R. H. Grubbs, *J. Organomet. Chem.* **1995**, *497*, 195–200; M. Mayr, B. Mayr, M. R. Buchmeiser, *Angew. Chem.* **2001**, *113*, 3957–3960; *Angew. Chem. Int. Ed.* **2001**, *40*, 3839–3842; L. R. Yang, M. Mayr, K. Wurst, M. R. Buchmeiser, *Chem. Eur. J.* **2004**, *10*, 5761–5770; C. Copéret, *New J. Chem.* **2004**, *28*, 1–10; F. Blanc, R. Berthoud, A. Salameh, J. M. Basset, C. Copéret, R. Singh, R. R. Schrock, *J. Am. Chem. Soc.* **2007**, *129*, 8434–8435; M. Chabanas, A. Baudouin, C. Copéret, J. M. Basset, *J. Am. Chem. Soc.* **2001**, *123*, 2062–2063; M. R. Buchmeiser, *Chem. Rev.* **2009**, *109*, 303–321.
[18] J. S. Kingsbury, A. H. Hoveyda, *J. Am. Chem. Soc.* **2005**, *127*, 4510–4517.
[19] X. Elias, R. Pleixats, M. Wong Chi Man, J. J. E. Moreau, *Adv. Synth. Catal.* **2006**, *348*, 751–762.
[20] X. Elias, R. Pleixats, M. Wong Chi Man, *Tetrahedron* **2008**, *64*, 6770–6781.
[21] X. Elias, R. Pleixats, M. Wong Chi Man, J. J. E. Moreau, *Adv. Synth. Catal.* **2007**, *349*, 1701–1713.
[22] A. Michrowska, R. Bujok, S. Harutyunyan, V. Sashuk, G. Dolgonos, K. Grela, *J. Am. Chem. Soc.* **2004**, *126*, 9318–9325.
[23] M. Zaja, S. J. Connon, A. M. Dunne, M. Rivard, N. Buschmann, J. Jiricek, S. Blechert, *Tetrahedron* **2003**, *59*, 6545–6558.
[24] K. Grela, S. Harutyunyan, A. Michrowska, *Angew. Chem.* **2002**, *114*, 4210–4212; *Angew. Chem. Int. Ed.* **2002**, *41*, 4038–4040.
[25] J. Handzlik, *J. Catal.* **2003**, *220*, 23–34; J. Handzlik, P. Sautet, *J. Catal.* **2008**, *256*, 1–14; J. Handzlik, P. Sautet, *J. Phys. Chem. C* **2008**, *112*, 14456–14463; J. Handzlik, *J. Phys. Chem. C* **2007**, *111*, 9337–9348.
[26] Y. D. Wu, Z. H. Peng, *J. Am. Chem. Soc.* **1997**, *119*, 8043–8049; E. Folga, T. Ziegler, *Organometallics* **1993**, *12*, 325–337; K. Monteyne, T. Ziegler, *Organometallics* **1998**, *17*, 5901–5907; H. H. Fox, M. H. Schofield, R. R. Schrock, *Organometallics* **1994**, *13*, 2804–2815; T. P. M. Goumans, A. W. Ehlers, K. Lammertsma, *Organometallics* **2005**, *24*, 3200–3206.
[27] A. Poater, X. Solans-Monfort, E. Clot, C. Copéret, O. Eisenstein, *J. Am. Chem. Soc.* **2007**, *129*, 8207–8216.
[28] X. Solans-Monfort, E. Clot, C. Copéret, O. Eisenstein, *J. Am. Chem. Soc.* **2005**, *127*, 14015–14025.
[29] L. Cavallo, *J. Am. Chem. Soc.* **2002**, *124*, 8965–8973.
[30] L. Cavallo, A. Correa, C. Costabile, H. Jacobsen, *J. Organomet. Chem.* **2005**, *690*, 5407–5413; C. Costabile, L. Cavallo, *J. Am. Chem. Soc.* **2004**, *126*, 9592–9600; S. E. Vyboishchikov, W. Thiel, *Chem. Eur. J.* **2005**, *11*, 3921–3935; C. Adlhart, P. Chen, *Angew. Chem.* **2002**, *114*, 4668–4671; *Angew. Chem. Int. Ed.* **2002**, *41*, 4484–4487; C. Adlhart, P. Chen, *Helv. Chim. Acta* **2003**, *86*, 941–949; S. Fomine, J. V. Ortega, M. A. Tlenkopatchev, *J. Mol. Catal. A* **2007**, *263*, 121–127; S. Fomine, J. V. Ortega, M. A. Tlenkopatchev, *J. Mol. Catal. A* **2005**, *236*, 156–161; S. Fomine, J. V. Ortega, M. A. Tlenkopatchev, *Organometallics* **2005**, *24*, 5696–5701; S. Fomine, M. A. Tlenkopatchev, *J. Organomet. Chem.* **2006**, *691*, 5189–5196; S. Fomine, S. M. Vargas, M. A. Tlenkopatchev, *Organometallics* **2003**, *22*, 93–99; G. Occhipinti, H. R. Bjørsvik, V. R. Jensen, *J. Am. Chem. Soc.* **2006**, *128*, 6952–6964; W. Janse van Rensburg, P. J. Steynberg, W. H. Meyer, M. M. Kirk, G. S. Forman, *J. Am. Chem. Soc.* **2004**, *126*, 14332–14333; A. C. Tsipis, A. G. Orpen, J. N. Harvey, *Dalton Trans.* **2005**, 2849–2858; C. E. Webster, *J. Am. Chem. Soc.* **2007**, *129*, 7490–7491; M. Jordaan, P. van Helden, C. van Sittert, H. C. M. Vosloo, *J. Mol. Catal. A* **2006**, *254*, 145–154; O. M. Aagaard, R. J. Meier, F. Buda, *J. Am. Chem. Soc.* **1998**, *120*, 7174–7182; R. J. Meier, O. M. Aagaard, F. Buda, *J. Mol. Catal. A* **2000**, *160*, 189–197.
[31] A. Correa, L. Cavallo, *J. Am. Chem. Soc.* **2006**, *128*, 13352–13353.
[32] S. E. Vyboishchikov, M. Bühl, W. Thiel, *Chem. Eur. J.* **2002**, *8*, 3962–3975.
[33] C. Adlhart, P. Chen, *J. Am. Chem. Soc.* **2004**, *126*, 3496–3510; M. Piacenza, I. Hyla-Kryspin, S. Grimme, *J. Comput. Chem.* **2007**, *28*, 2275–2285.
[34] B. F. Straub, *Adv. Synth. Catal.* **2007**, *349*, 204–214; W. J. van Rensburg, P. J. Steynberg, M. M. Kirk, W. H. Meyer, G. S. Forman, *J. Organomet. Chem.* **2006**, *691*, 5312–5325.
[35] C. Adlhart, C. Hinderling, H. Baumann, P. Chen, *J. Am. Chem. Soc.* **2000**, *122*, 8204–8214.
[36] I. C. Stewart, D. Benitez, D. J. O'Leary, E. Tkatchouk, M. W. Day, W. A. Goddard, R. H. Grubbs, *J. Am. Chem. Soc.* **2009**, *131*, 1931–1938.
[37] Y. Chauvin, *Angew. Chem.* **2006**, *118*, 3824–3831; *Angew. Chem. Int. Ed.* **2006**, *45*, 3740–3747; J.-L. Hérisson, Y. Chauvin, *Makromol. Chem.* **1971**, *141*, 161–176.
[38] A. Comas-Vives, C. González-Arellano, A. Corma, M. Iglesias, F. Sánchez, G. Ujaque, *J. Am. Chem. Soc.* **2006**, *128*, 4756–4765.
[39] A. D. Becke, *J. Chem. Phys.* **1993**, *98*, 5648–5652; C. T. Lee, W. T. Yang, R. G. Parr, *Phys. Rev. B* **1988**, *37*, 785–789.
[40] Gaussian 03, Revision E.01 M. J. Frisch, G. W. Trucks, H. B. Schlegel, G. E. Scuseria, M. A. Robb, J. R. Cheeseman, J. A. Montgomery, Jr., K. N. Kudin, J. C. Burant, J. M. Millam, S. S. Iyengar, J. Tomasi, V. Barone, B. Mennucci, M. Cossi, G. Scalmani, N. Rega, G. A. Petersson, H. Nakatsuji, M. Hada, M. Ehara, K. Toyota, R. Fukuda, J. Hasegawa, M. Ishida, T. Nakajima, Y. Honda, O. Kitao, H. Nakai, M. Klene, X. Li, J. E. Knox, H. P. Hratchian, J. B. Cross, C. Adamo, J. Jaramillo, R. Gomperts, R. E. Stratmann, O. Yazyev, A. J. Austin, R. Cammi, C. Pomelli, J. W. Ochterski, P. Y. Ayala, K. Morokuma, G. A. Voth, P. Salvador, J. J. Dannenberg, V. G. Zakrzewski, S. Dapprich, A. D. Daniels, M. C. Strain, O. Farkas, D. K. Malick, A. D. Rabuck, K. Raghavachari, J. B. Foresman, J. V. Ortiz, Q. Cui, A. G. Baboul, S. Clifford, J. Cioslowski, B. B. Stefanov, G. Liu, A. Liashenko, P. Piskorz, I. Komaromi, R. L. Martin, D. J. Fox, T. Keith, M. A. Al-Laham, C. Y. Peng, A. Nanayakkara, M. Challacombe, P. M. W. Gill, B. Johnson, W. Chen, M. W. Wong, C. Gonzalez, J. A. Pople, Gaussian Inc., Pittsburgh PA, **2003**.
[41] W. Küchle, M. Dolg, H. Stoll, H. Preuss, *Mol. Phys.* **1991**, *74*, 1245–1263.
[42] A. W. Ehlers, M. Böhme, S. Dapprich, A. Gobbi, A. Höllwarth, V. Jonas, K. F. Köhler, R. Stegmann, A. Veldkamp, G. Frenking, *Chem. Phys. Lett.* **1993**, *208*, 111–114.
[43] M. M. Francl, W. J. Pietro, W. J. Hehre, J. S. Binkley, M. S. Gordon, D. J. Defrees, J. A. Pople, *J. Chem. Phys.* **1982**, *77*, 3654–3665; W. J. Hehre, R. Ditchfield, J. A. Pople, *J. Chem. Phys.* **1972**, *56*, 2257–2261.
[44] P. C. Hariharan, J. A. Pople, *Theor. Chim. Acta* **1973**, *28*, 213–222.
[45] Y. Zhao, N. E. Schultz, D. G. Truhlar, *J. Chem. Theory Comput.* **2006**, *2*, 364–382; Y. Zhao, D. G. Truhlar, *Acc. Chem. Res.* **2008**, *41*, 157–167.
[46] Gaussian 09, Revision A.2, M. J. Frisch, G. W. Trucks, H. B. Schlegel, G. E. Scuseria, M. A. Robb, J. R. Cheeseman, G. Scalmani, V. Barone, B. Mennucci, G. A. Petersson, H. Nakatsuji, M. Caricato, X. Li, H. P. Hratchian, A. F. Izmaylov, J. Bloino, G. Zheng, J. L. Sonnenberg, M. Hada, M. Ehara, K. Toyota, R. Fukuda, J. Hasegawa, M. Ishida, T. Nakajima, Y. Honda, O. Kitao, H. Nakai, T. Vreven, J. A. Montgomery, Jr., J. E. Peralta, F. Ogliaro, M. Bearpark, J. J. Heyd, E. Brothers, K. N. Kudin, V. N. Staroverov, R. Kobayashi, J. Normand, K. Raghavachari, A. Rendell, J. C. Burant, S. S. Iyengar, J. Tomasi, M. Cossi, N. Rega, N. J. Millam, M. Klene, J. E. Knox, J. B. Cross, V. Bakken, C. Adamo, J. Jaramillo, R. Gomperts, R. E. Stratmann, O. Yazyev, A. J. Austin, R. Cammi, C. Pomelli, J. W. Ochterski, R. L. Martin, K. Morokuma, V. G. Zakrzewski, G. A. Voth, P. Salvador, J. J. Dannenberg, S. Dapprich, A. D. Daniels, Ö.

Farkas, J. B. Foresman, J. V. Ortiz, J. Cioslowski, D. J. Fox, Gaussian, Inc., Wallingford CT, **2009**.
[47] D. Benitez, E. Tkatchouk, W. A. Goddard, *Chem. Commun.* **2008**, 6194–6196.
[48] Y. Zhao, D. G. Truhlar, *Org. Lett.* **2007**, *9*, 1967–1970.
[49] V. Barone, M. Cossi, J. Tomasi, *J. Chem. Phys.* **1997**, *107*, 3210–3221; S. Miertuš, E. Scrocco, J. Tomasi, *Chem. Phys.* **1981**, *55*, 117–129.
[50] A. A. C. Braga, G. Ujaque, F. Maseras, *Organometallics* **2006**, *25*, 3647–3658.
[51] T. Tuttle, D. Q. Wang, W. Thiel, *Organometallics* **2006**, *25*, 4504–4513.
[52] D. Ardura, R. Lopez, T. L. Sordo, *J. Phys. Chem. B* **2005**, *109*, 23618–23623.
[53] B. O. Leung, D. L. Reid, D. A. Armstrong, A. Rauk, *J. Phys. Chem. A* **2004**, *108*, 2720–2725.
[54] S. Sakaki, T. Takayama, M. Sumimoto, M. Sugimoto, *J. Am. Chem. Soc.* **2004**, *126*, 3332–3348.
[55] J. Cooper, T. Ziegler, *Inorg. Chem.* **2002**, *41*, 6614–6622.
[56] M. Bieniek, A. Michrowska, D. L. Usanov, K. Grela, *Chem. Eur. J.* **2008**, *14*, 806–818.
[57] J. A. Love, J. P. Morgan, T. M. Trnka, R. H. Grubbs, *Angew. Chem.* **2002**, *114*, 4207–4209; *Angew. Chem. Int. Ed.* **2002**, *41*, 4035–4037.
[58] K. Vehlow, S. Maechling, S. Blechert, *Organometallics* **2006**, *25*, 25–28.
[59] C. H. Suresh, M. H. Baik, *Dalton Trans.* **2005**, 2982–2984; C. H. Suresh, N. Koga, *Organometallics* **2004**, *23*, 76–80; P. E. Romero, W. E. Piers, *J. Am. Chem. Soc.* **2007**, *129*, 1698–1704; P. E. Romero, W. E. Piers, *J. Am. Chem. Soc.* **2005**, *127*, 5032–5033.
[60] J. Feldman, W. M. Davis, R. R. Schrock, *Organometallics* **1989**, *8*, 2266–2268; J. Feldman, W. M. Davis, J. K. Thomas, R. R. Schrock, *Organometallics* **1990**, *9*, 2535–2548; F. Blanc, R. Berthoud, C. Copéret, A. Lesage, L. Emsley, R. Singh, T. Kreickmann, R. R. Schrock, *Proc. Natl. Acad. Sci. USA* **2008**, *105*, 12123–12127.
[61] A. M. Leduc, A. Salameh, D. Soulivong, M. Chabanas, J. M. Basset, C. Copéret, X. Solans-Monfort, E. Clot, O. Eisenstein, V. P. W. Böhm, M. Röper, *J. Am. Chem. Soc.* **2008**, *130*, 6288–6297.
[62] A. R. Rossi, R. Hoffmann, *Inorg. Chem.* **1975**, *14*, 365–374.
[63] M. Barbasiewicz, A. Szadkowska, A. Makal, K. Jarzembska, K. Wozniak, K. Grela, *Chem. Eur. J.* **2008**, *14*, 9330–9337.

Received: December 22, 2009
Published online: May 12, 2010

